Retrieving CH4 Emissions from Coal sampled with UAV-based Aircore system by using GA-IPPF model

Tianqi Shi[1], Zeyu Han[2], Ge Han [3],Xin Ma[1*],Huilin Chen[4,5]*, Truls Andersen[5], Huiqin Mao[6],Cuihong Chen[6],Haowei Zhang[1],Wei Gong[1,7]

[1] State Key Laboratory of Information Engineering in Surveying, Mapping and Remote Sensing, Wuhan University, Luoyu Road No.129, Wuhan 430079, China;
[2]School of Mathematics and Statistics, Wuhan University, Luoyu Road No.129, Wuhan 430079, China;
[3] School of Remote Sensing and Information Engineering, Wuhan University, Luoyu Road No.129, Wuhan 430079, China;
[4]Joint International Research Laboratory of Atmospheric and Earth System Sciences, School of Atmospheric Sciences, Nanjing University, Nanjing, China;
[5]Centre for Isotope Research, Energy and Sustainability Institute Groningen (ESRIG), University of Groningen, Groningen, Netherlands;
[6]Ministry of Ecology and Environment Center for Satellite Application on Ecology and Environment, Beijing, China;
[7] Electronic Information School, Wuhan University, Luoyu Road No.129, Wuhan 430079,China;

Correspondence to: Xin Ma(maxinwhu@whu.edu.cn); Huilin Chen (huilin.chen@rug.nl)

Abstract

Quantifying CH4 emissions from coal mines has large uncertainty owing to the lack of effective monitoring methods. In this study, we developed a genetic algorithm–interior point penalty function (GA-IPPF) model to calculate the emission rate of large point sources of CH4. This model can provide the detailed optimized dispersion parameters and has self-calibration characteristics that reduce the accuracy requirements for auxiliary data. We evaluate the influence of different parameters on the retrieved CH4-emission rate by the GA-IPPF, including the uncertainty of CH4 concentration measurements, number of CH4 measurements, and meteorological data. Furthermore, based on the atmospheric CH4 concentration measurements downwind of a Pniówek coal-mine ventilation shafts from a UAV-based AirCore system and the GA-IPPF model, we retrieve the CH4-emission rates from the Pniówek coal (Silesia coal mining region mine, Poland) ventilation shaft. Results show that the CH4-emission rates are variable even in a single day, ranging from 5.6±0.2 kt/year to 12.4±0.6 kt/year on August 18, 2017 and from 3.0±0.3 kt/year to 12.7±0.5 kt/year on August 21, 2017. The combination of the flexible UAV-based AirCore CH4 measurements and the robust GA-IPPF model provides a effective means of quantifying CH4 emissions from coal mines.

1.Introduction

The release of CH_4 into the atmosphere during coal mining is very concerning because it contributes to increased atmospheric concentration of CH_4, one of the most important greenhouse gases and waste resources(Cardoso-Saldana and Allen 2020; Zhang et al. 2020). However, CH_4 emissions during coal mining are not always stable owing to collection or manufacturing processes, weather fluctuations, terrain effects(Nathan et al. 2015b). Bottom-up inventories could provide us with approximate information on CH_4-emission rates from strong sources. However, inventories cannot serve as a standard for formulating policies to reduce anthropic CH_4 emission because of their low temporal resolution and uncertainty. The temporal resolution and accuracy of bottom-up inventory are too low to obtain emission

information instantaneously(Liu et al. 2020; Pan et al. 2021). Based on the measurements of CH_4 concentration around the emission source, developing a fast retrieval model to obtain emission intensity is an acceptable method. With the development of remote-sensing technologies, the CH_4 emission rate has become possible to quantify based on CH_4 concentration samples or measurement.

Greenhouse gases observing satellite and TROPOspheric Monitoring Instrument could obtain the column concentration of CH_4 (XCH_4, ppb) with a spatial resolution of 10 km×10 km and 5 km×7.5 km. The regional CH_4 flux could be retrieved by assimilating the measured XCH_4 into an atmospheric dispersion model(Feng et al. 2016; Tu et al. 2022). PRISMA hyperspectral imaging satellite and GHGsat could detect increased CH_4 caused by strong emission sources with high spatial resolution, and the comprehensive CH_4 emission could be quantified by integrated mass enhancement or cross-sectional flux method(Guanter et al. 2021; Varon et al. 2020). However, CH_4 emission from coal is not constant even in a short time, and the spatial and temporal resolutions of satellites are not allowed to repeat the quantification of CH_4 emission from coals in the same day(Schneising et al. 2020; Varon et al. 2019). An airborne platform could fly in low altitude to improve the acquisition of CH_4 concentration(Elder et al. 2020; Wolff et al. 2021a) and estimate CH_4 emission from strong sources by cross-sectional flux method or Gaussian dispersion method. However, it has strict requirements for the flight track (downwind direction) and amount of measured CH_4 concentration data. Most ground-based sensors have the advantage to sample the concentration around the source continuously, but it could collect data only near the surface or could only measure column concentration(Caulton et al. 2017; Robertson et al. 2017; Zhou et al. 2021), which are insufficient to generate the distribution characteristic of the emission source. Ground-based different-absorption LIDAR could obtain the CH_4 profile concentration in different altitudes, which is suitable as the input of the emission-retrieval model(Shi et al. 2020a), but it has high requirements in terms of performance of hardware and system stability(Shi et al. 2020b). An unmanned aerial vehicle (UAV) could reach any location rapidly around the CH_4 sources, which could sample CH_4 concentration with location information(Iwaszenko et al. 2021; Nathan et al. 2015b), when equipped with an in-situ gas sensor. It could also acquire the characteristic of distribution with adequate data, which is beneficial to retrieving the emission rate.

Mass-balance method has been applied in determining CH_4 emissions based on UAV-based samples(Allen et al. 2018). Emission rates calculated by this method contain large uncertainty because the main kernel is Kriging interpolation(Nathan et al. 2015a), which causes obvious uncertainty in representing the actual feature of diffusion. The Gaussian dispersion model has also been applied in retrieving gas emission from strong sources(Shah et al. 2019)[30], and is used to quantify CH_4 emission from a coal-mine ventilation shaft in this study. However, existing emission-retrieval models need priori information on diffusion parameters to retrieve the emission rate. Moreover, the accuracy of measurements of auxiliary meteorological data influences the result of CH_4-emission calculation. Therefore, we develop herein a model to overcome these shortcomings. Our model could calculate the diffusion parameters without prior information and reduce the impact of meteorological data on the calculated CH_4-emission rate.

In the present study, we collected CH_4 concentration data around a coal-mine ventilation shaft by using UAV-based active AirCore system with high accuracy(Andersen et al. 2018) for a total of seven Flights. Then, a CH_4 emission-retrieval model based on genetic algorithm (GA) combined with interior point-penalty function (IPFF) is presented. GA-IPPF could help us obtain detailed information on emission intensity and diffusion parameters. Finally, the performance of GA-IPPF model is compared with other quantification methods for CH_4 emission.

Poor English and not clear - you mean that the orbital pattern of the satellite means that they do not pass over the same area twice within the same day.

I presume you mean fixed location. This is also dependent on wind direction, so the emission will not be sampled all of the time, unless monitoring is inside of the source.

Accuracy of what? AirCore only collects the sample so presumably GPS location X,Y,Z co-ordinates at high frequency.

2.Data and methods

2.1.Active AirCore System

The active AirCore system comprises a ~50 m coiled stainless-steel tube that works in conjunction with a micropump and a small pinhole orifice (45 μm) to sample air along the trajectory of a drone. As long as the pressure downstream of the orifice is more than half of that of the upstream (ambient) pressure, a critical flow through the orifice is obtained. This finding means that the flow rate depends only on two variables, namely, the air temperature and the upstream (ambient) pressure, both of which are monitored during the flight. After obtaining the air sample, the sample is analyzed on a cavity ring down Spectrometer model G2401-m for CO_2, CH_4, and CO. For CH_4, the accuracy of samples is ±0.02 parts per million (ppm). The active AirCore system is controlled using an Arduino-built data logger, which records the temperature inside the carbon fiber housing. It also records the ambient temperature, ambient pressure, relative humidity, and pressure downstream of the pinhole orifice to ensure that critical flow is achieved. The datalogger also logs the GPS coordinates. The weight of the active AirCore system is ~1 kg. The active AirCore system is attached to a DJI Inspire Pro 1, which is capable of providing flights of ~12 min.

Need to be clear that the AirCore sample is removed from the drone and replayed through the Picarro on the ground

Samples are not accurate, measurements are, but I presume that the reference here is to precision not accuracy, as you need instrument calibration to measure accuracy.

2.2. Meteorological measurements

A radiosonde (Sparv Embedded AB, Sweden, model S1H2-R) measures ambient temperature, ambient pressure, ambient relative humidity, wind speed, and wind direction. The detection range of the temperature sensor is –40 °C to +80 °C, with an accuracy of 0.3 °C. The pressure sensor has a detection range of 300–1100 mbar, with an accuracy of 1 mbar. The relative humidity sensor measures a range of 0%–100%, with an accuracy of approximately 2%. Owing to the good connection between the radiosonde and satellites, we assume that the uncertainty in the wind direction is low. The wind speed can be estimated within a range of 0–150 m/s, with an uncertainty of approximately 5%. If the wind-speed reading is less than 4 m/s, a minimum uncertainty of 0.2 m/s is given. The radiosonde is lifted by a ~30 L helium-filled balloon and is tethered onto a fishing line for easier retrieval after making a vertical profile.

2.3 Emission retrieve model

2.3.1.Gaussian dispersion model

The Gaussian dispersion model is used to analyze the CH_4 fugitive from the coal mine in this work. The location of emission source is regarded as the coordinate origin; X-axis is the direction of the downwind, Y-axis is cross-wind direction, and Z-axis is the altitude above the ground. Based on the established coordinate system, the Gaussian plume could be modeled by Equation 1:

$$C(x,y,z)=\frac{q}{2\pi u\sigma_y\sigma_z}\exp(\frac{-(y)^2}{2\sigma_y^2})\left\{\exp(\frac{-(z-H)^2}{2\sigma_z^2})+\alpha\cdot\exp(\frac{-(z+H)^2}{2\sigma_z^2})\right\}+B \quad (1)$$

$$\sigma_y=a\cdot x^b \quad (2)$$

$$\sigma_z=c\cdot x^d \quad (3)$$

methane is being emitted not coal

C is the concentration (g/m^3), q (g/s) is the emission rate of coal from stack, u is the mean wind speed around the stack (m/s), H is the effective stack height, σ_y is the dispersion coefficient in the horizontal direction, σ_z is the dispersion coefficient in the vertical direction, u is the wind speed (m/s), and B is the background concentration of CH_4. Moreover, α is the reflection index of this phenomenon; and x, y, and z are the positions of the samples in the determined coordinate system.

2.3.2.GA-IPPF model.

First, the genetic algorithm (GA) kernel calculates Q and other dispersion parameters as first guess(Liu

and Michalski 2016). It guarantees the retrieved unknown parameters through the global optimum solution, including Q and diffusion parameters, as shown in Figure1.Then, the results calculated by GA serve as oral input parameters and constraints in the IPPF model, and actual values of the concerned parameters are retrieved by IPPF.

what do you mean by oral?

Based on the Gaussian dispersion model, auxiliary meteorological data, location information, and CH_4 samples, we determine the unknown parameters in equations 1 to 3 by using GA, including q, H, a, b, c, d, and α. First, the locations and concentration of CH_4 samples and wind serve as an initial input of equation 1. Then, the fitness value evaluates the applicability of the calculated parameters in each step. We define the fitness value as

$$F = \sum_{i=1}^{n} (C_m^i - C_s^i)^2 \tag{4}$$

$$C_s^i(x,y,z) = \sum_{i=1}^{n} \frac{q'}{2\pi u' \sigma_y' \sigma_z'} \exp\left(\frac{-(y)^2}{(\sigma_y')^2}\right)\left\{\exp\left(\frac{-(z-H')^2}{(\sigma_z')^2}\right) + \alpha' \cdot \exp\left(\frac{-(z+H')^2}{(\sigma_z')^2}\right)\right\} + B' \tag{5}$$

F is the fitness value; C_m^i is the sample CH_4 concentration; i is the number of samples; C_s^i is the simulated concentration of CH_4 in the location of samples calculated by formula 5; and q′, u′, σ_y', σ_z', H′, α′, and B′ are the calculated CH_4-emission rate, wind speed, diffusion parameters, emission height, reflect index, and background CH_4 concentration, respectively, acquired from the "Mutation" in Figure1. When f is less than the threshold value (1×10^{-5}) of the fitness value, the corresponding parameters are treated as the results of output.

IPPF rebuilds the inequality constraint conditions to the unconstrained solution process. It forces the start point to satisfy the constraints, as shown in formula 6.

$$minF\left(x, r_k\right) = f(x) + r_k B(x) \tag{6}$$

f(x) is the unconstrained equation, and r_k is the coefficient of the constrained equation B(x).When the solution parameters are out of the constraints, $r_k B(x)$ is large, thereby ensuring that the final solution is feasible under the inequality constraint conditions.

To obtain the inequality constraints, GA is repeated 1000000 times, and the mean values of the calculated wind speed, wind direction, H, a, b, c, d, and α are treated as the oral input of IPPF model. The domains of H, a, b, c, d, and α are determined by two times the standard deviation of the corresponding results in GA. The constraint values of wind speed and direction are set according to the precision of actual measurements, m±σ, whereas m is the measured value of wind speed or wind direction, and σ is their precision. Actual B values are considered to range within 1800–2500 ppb. Then, the Pearson correlation coefficient (R) values of the actual samples and simulated one work as judgment in the solution process of formula 7.

$$R = \frac{\sum_{i=1}^{n}\left(C_s^i - \overline{C_s}\right)\left(C_m^i - \overline{C_m}\right)}{\sqrt{\sum_{i=1}^{n}\left(C_s^i - \overline{C_s}\right)^2}\sqrt{\sum_{i=1}^{n}\left(C_m^i - \overline{C_m}\right)^2}} \tag{7}$$

The results are treated as the final retrieved values of the concerned parameters when the R reaches the maximum. We use the "fmincon (interior point)" toolbox in MATLAB 2020a to implement the IPPF model.

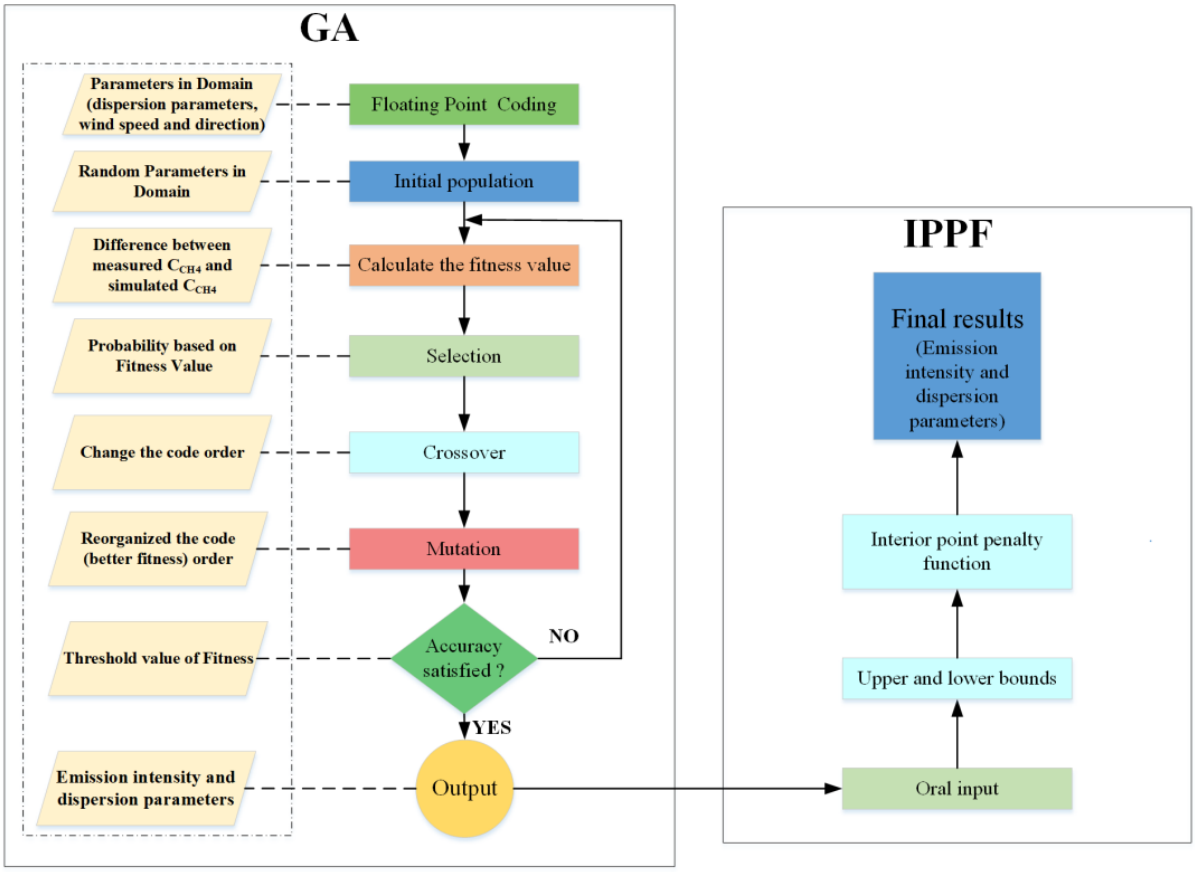

Figure1. Flow chart of Genetic Algorithm and IPPF model.

This section needs to go before the model section as the location is mentioned. You should also make it clear what type of source this is as this will make a big difference to the model. Is a a large open coal pit, or emission from a deep mine shaft or vent, or is it a combination of both.

2.4.Measurement Site

The Pniówek coal mine (49.975° N, 18.735° E) is a large mine in south Poland in Pniówek, Silesian Voivodeship, which is 190 km southwest of the capital Warsaw, see Figure2. It has a large coal reserve estimated to be about 101.3 million tons. Its coal production is about 5.16 million tons per year.

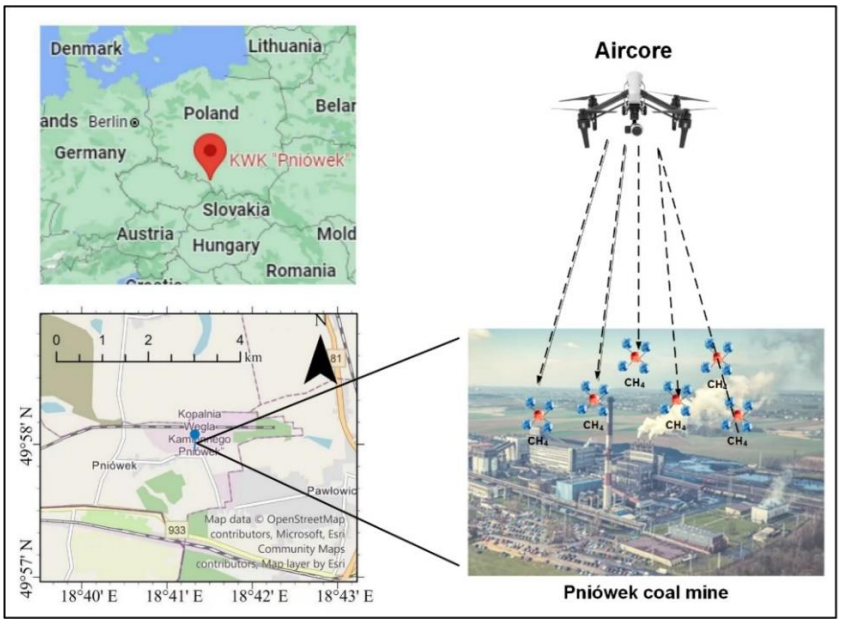

Figure2. The Pniówek coal mine

Caption needs more explanation. What actually is the zoomed map showing? Where is the mine? Is pink the mine buidlings? is it deep mine with shaft or open pit?

3. Results

3.1. Validation of performance of GA-IPPF model through simulations

What is a coal?

First, the dispersion of CH_4 emission from a coal is simulated by equation 1, and the dispersion parameters are shown in Table 1. To make the simulations close to the actual measurement scenarios, random errors are added to the CH_4 concentration samples (5%), wind speed (± 0.3 m/s), and wind direction (± 20°). The spatial resolution of the supposed samples is 10 m, and 70 samples are selected from the simulated dispersion to represent the data acquired by the UAV-based AirCore. Then, the concerned parameters are retrieved by the GA-IPPF method. The input parameters include hypothetical wind speed, wind direction, and 70 samples, as shown in Figure3. Simulations are repeated 10 000 times, and the average values of the corresponding parameters are treated as the "Retrieved" results in Table 1.

Showing simulated data without showing any real 3-D data from the AirCore. What does this look like? What are you trying to simulate?

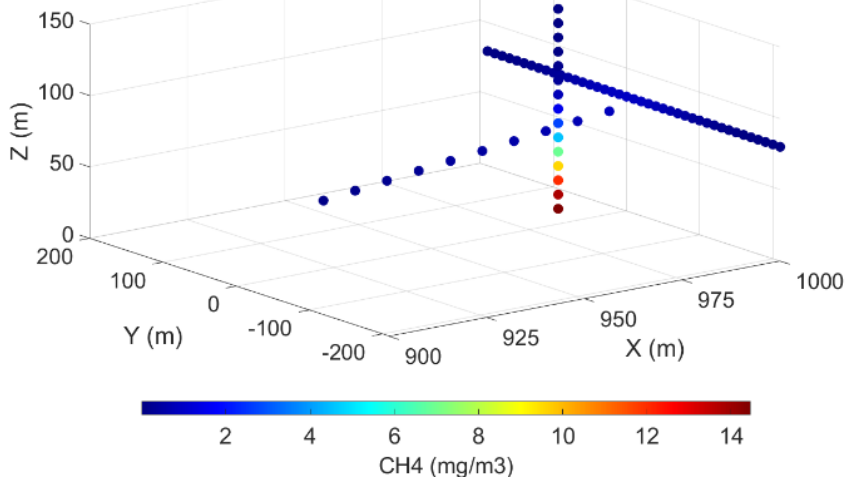

Figure3. The determined 70 CH_4 samples in simulations

Table 1.Set parameters in dispersion simulation and the retrieved results

Parameters	Actual	Retrieved
Emission intensity (g/s)	300	300.5±0.01
Wind speed (m/s)	3	3±0.01
Wind direction (°)	90	90±0.01
a	0.11	0.13±0.02
B	0.9	0.9±0.02
c	0.1	0.12±0.01
d	0.82	0.8±0.01
B (ppb)	1900	1900±3
Emission height (m)	20	19.7±1.2
α	0.9	0.89±0.03

"Actual" means the set values of parameters, and "Retrieved" means the average values of parameters retrieved by GA-IPPF model through 10 000 times of simulation.

Show which is q in Table 1

As shown in Table 1, q retrieved by GA-IPPF has only 0.17% bias compared with the set values. Emission height only has 0.3 m bias to set one, and uncertainty is only 0.6% to 20 m. Other retrieved parameters also show high consistency with the original settings.

3.2. Stability analyses

The necessary input parameters in GA-IPPF contain meteorological data (wind speed and direction), accuracy of CH_4 samples, and amount of CH_4 samples. In formula 1, wind speed nearly has a linear relationship with the emission estimation. Wind speed is also an important factor that determines

atmospheric stability according to the Pasquill–Gifford method(Venkatram 1996) as it affects the diffusion parameters of σ_y and σ_z. The coordinate is built according to the wind direction, which is defined the plane coordinates of CH_4 samples. According to formulas 2 to 3, errors in wind-direction measurement lead to wrong σ_y and σ_z on each position of samples. CH_4 samples are the most important factors to determine the Gaussian diffusion. The accuracy of samples influences the judgment of "fitness" in the GA process. More samples collected in different positions help rebuild the spatial-distribution characteristics of the plume because it provides larger possibility for fitting process in IPPF and helps determine the optimum solution. To evaluate the influence of errors in the measurements of necessary parameters on the final retrieved results, the same settings in Table 1 are used as actual results. The performance of the GA-IPPF model with additional random errors in each parameter are simulated 10 000 times, as shown in Figure4.

something is missing here

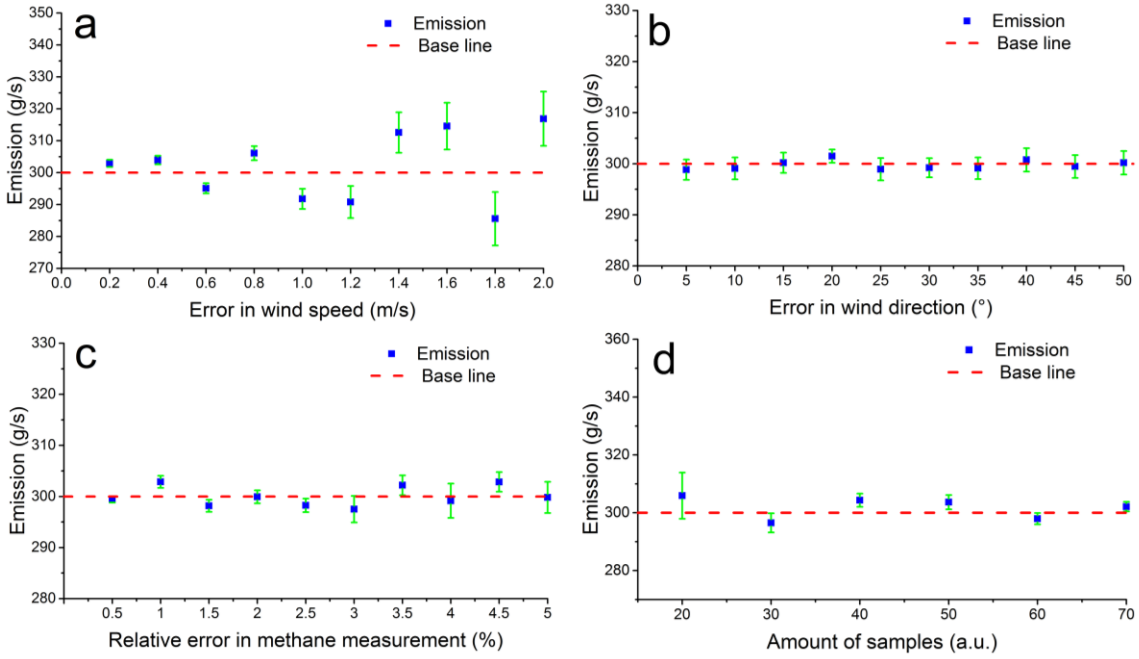

Figure4. Influence of accuracy of parameters on final results. Baseline represents the set emission rate of CH_4, 300 g/s: (a) wind speed, with additional error ranging within 0.2–2 m/s and an interval of 0.1 m/s, (b) wind direction, with additional error ranging within 5°–40° and an interval of 5 °, (c) accuracy of CH_4 samples, with additional error ranging within 0.5%–5.0% and an interval of 0.5%, and (d) amount of CH_4 samples, randomly selected as 20–70 among the defined 70 samples.

Need to make clear earlier that q = emissions in g/s

In Figure 4 (a), the mean value of q retrieved by GA-IPPF has nearly the same with the baseline if the error in wind speed is less than 0.4 m/s and the maximum bias to the baseline is 16.3 g/s. Fluctuation of q occurs obviously if error in wind speed exceeds 0.4 m/s. The standard errors of q are positively correlated with the values of errors in wind speed, indicating that the accuracy of wind-speed measurements largely influences the stability of the GA-IPPF model. This model has a self-adjustment function for wind speed; for example, when the oral wind speed is 3 m/s, the maximum standard error of q is only 8.5 g/s (3.5% to the 300 g/s) when the additional error of wind is 2 m/s (66.7% to 3 m/s).

The retrieved q shows less sensitivity on errors in wind direction, see Figure4(b). When errors in the wind direction are 5° to 40°, all biases of q are within 1.1 g/s and the standard errors are around 2.3 g/s. Wind direction determines the spatial location of the sampling point, and wrong location information leads to distinct errors in emission estimation. GA-IPPF shows highly accurate ability in wind direction

This implies that there could be big errors in q if the source is not a point source, but unequally distributed over an area, which could be the case with a farm or landfill site emission.

to obtain the global optimum solution.

Sampling accuracy has small impact on the retrieved q within different settings in CH_4 samples' accuracy, see Figure4(c). Standard deviation is positively correlated with errors in CH_4 measurements. The standard deviation is 3.1 g/s when the measurement error reaches 5%. Notably, the uncertainty of CH_4 samples measured by UAV-based AirCore system is far less than 5%. The AirCore system could acquire more than 70 CH_4 samples in actual feasible measurements, thereby guaranteeing the accuracy of the retrieved CH_4 emission by coal to exceed 99.2%.

How do you know these are errors and not limitations of instrument precision?

Not clear what this means. Number of air Core samples that can be collected and analysed within a given time period within the same source emission plume

The number of measurement points obviously influences the final accuracy of q by the GA-IPPF model, see Figure4(d). It has 5.9 g/s bias to 300 g/s when n is 20. The accuracy of q and the standard error are negatively correlated with n, which provides the number of judging criteria for the fitting process in the retrieval model. Hence, n directly influences the retrieved results. The AirCore system has the advantage of continuous sampling during flight, which integrates the atmospheric signals along the flight path and helps reduce the uncertainty of the retrieved q. On the other hand, the smoothing of the atmospheric signal also reduces the spatial resolution of the measurements, which needs to be considered during the optimization[30].

IPPF can suitably solve the problem of inequality constraints, and the calculated solution guarantees the calculated parameters to be within the feasible region. In this section, GA-IPPF model performance and its adjustments on the concerned four input parameters were discussed.

are

3.3. Actual experiments

Fifteen active AirCore flights around Pniówek coal mine are collected successfully on August 18, 2017 and August 21, 2017. The sample data in Flight 8 (18/8/2017) and Flight 15 (21/8/2017) are used to evaluate the GA-IPPF model, as shown in Figure5.

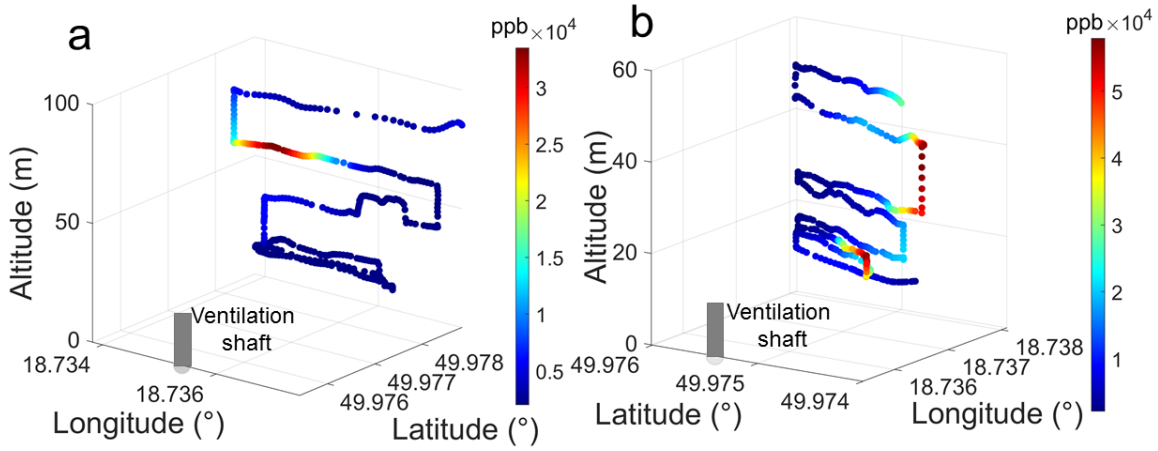

Says Flight 8 in text above

Figure5. Samples of CH_4 in two Flights: (a) Flight 6 and (b)Flight 15.

In Flight 5, the AirCore system collects CH_4 around the coal spirally from 0 m to 98 m, for a total of 376 samples, and the measurement period is 7 min, ranging from 1980.1 ppb to 49 113.9 ppb. In Flight 15, the AirCore system collects a total of 400 samples, and the measurement period is 9 min, ranging from 2131.7 ppb to 57 265.3 ppb. Both Flights show high spatial variability in CH_4 exhaust from coal mine. Subsequently, we input the wind speed, wind direction, location information, and CH_4 samples collected from Flights into the GA-IPPF model. To express the final retrieved emission (Q) in g/s, the dry-air mixing ratio of CH_4 C (ppb) is transformed into mass concentration m (g/m^3) as follows:

in a spiral pattern

The Picarro measurement rate doesn't change so why 376 measurements in 7 minutes and 400 in 9 minutes?

$$m = C \cdot \frac{M_{CH4}}{M_{Air}} \tag{8}$$

Surely an AirCore is one sample that has enough air to allow 400 measurements when attached to the Picarro?

M_{CH4} is the molar mass of CH_4, M_{air} is the molar mass of air.

The retrieved results are shown in Table 2. Notably, the emission height in Flight 15 is larger than that of Flight 6, which may be caused by the difference in thermal energy and vertical wind speed of the two flights. The background concentrations of CH_4 are 2001.3 and 2002.1 ppb in Flights 6 and 15, respectively, which show little difference. The dates of the two Flights are very close, so the background concentration of CH_4 in two days have nearly the same seasonal characteristic. The exhaust gases of coal mine are emitted through the stack with effective emission heights of 5.7 and 3.64 m, respectively.

Why is the calculated emission height an order of magnitude higher in the model results?

To evaluate the rationality of the retrieved results, these parameters are used to simulate CH_4 diffusion from the Pniówek coal mine according to equation 1. The comparison between simulated CH_4 concentration and actual samples in the same locations is shown in Figure6.

Table 2. Results calculated by GA-IPFF model

Parameters	Flight 6	Flight 15
Oral wind speed (m/s)	4.5	4.1
Oral wind direction (°)	310	125.4
Emission intensity (kt/year)	6.1±0.3	8.4±0.5
Wind speed (m/s)	3.25	3.20
Wind direction (°)	349.6°	128.1
a	0.22	0.31
b	0.90	0.90
c	0.006	1.50
d	1.29	0.38
B (mg/m^3)	1.55	1.57
Emission height (m)	59.3	36.3
Reflection index	0.85	1.0

Then, we also calculated the difference between the actual measured points and simulated ones as

$$D_c = C_s - C_m \quad (9)$$

D_c is the difference of CH_4 concentration between actual measured and simulated ones. C_s is simulated CH_4 concentration (mg/m^3),C_m is simulated CH_4 concentration (mg/m^3).

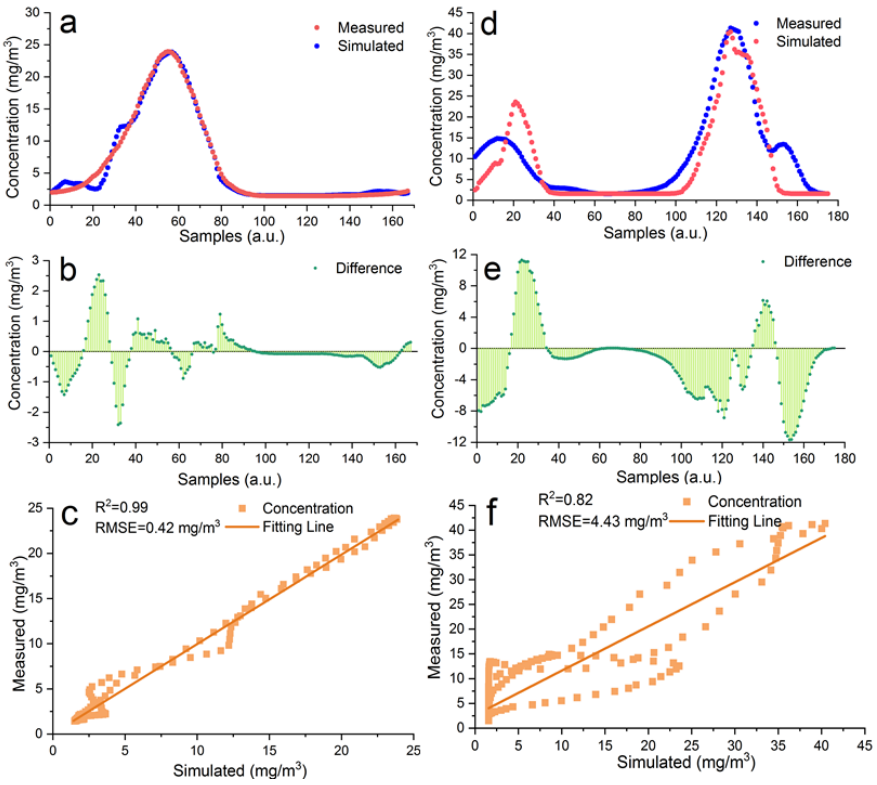

Figure6. Comparison between the measured samples and the simulated ones based on the parameters in Table 1: (a). Flight 6 and (d) Flight 15. The difference of simulated CH4 concentration and actual measured ones:(b) Flight 6 and (e)Flight 15. Correlation Analysis: (c) Flight 6 and (f)Flight 15.

As shown in Figure6(a), the tendency of the simulated concentration data is consistent with the measured ones in Flight 6. The largest value (NO.55) of the measured CH4 concentration is 23.9 mg/m3, whereas simulated one is 23.8 mg/m3 on same location, only 0.42% bias. Dc is ranging from -2.4 to 2.3 mg/m3 in Flight 6 (see Figure6(b)), this little bias indicates the simulated result is reasonable. The R2 of the measured samples and simulated ones is 0.99, root mean square error (RMSE) is 0.42 mg/m3.It indicates the GA-IPPF model could correctly rebuild the diffusion of CH_4 in Flight 6. Figure6(d) shows a slight difference between the two items in the first peak and third peak. Since the GA-IPPF method would adjust more weights to the samples with higher concentration (NO.100 to 150 in Flight 15) to get the global optimal solution of the relevant parameters, this would lead to the low fitness of the first peak in Figure6(e). In general, the tendency of the simulated ones remains consistent with that of the actual samples in Flight 15, especially for the points in the second peak. R2 and RMSE of the measured samples and simulated ones in Flight 15 also show the high applicability of the retrieved parameters.

Do you mean 'assign more weighting'?

3.4. Uncertainty Analyses

The uncertainties in CH_4-emission estimations are derived from the measurements of meteorological data and CH_4 samples in the discussed Flights. As shown in Figure3, n is the largest source that contributes to the uncertainty in emission calculation, and the accuracy of AirCore samples, wind speed, and wind direction should also be of concern. Therefore, the total uncertainty in actual CH_4 emission retrieved could be calculated as

$$\varepsilon_t = \sqrt{\varepsilon_n^2 + \varepsilon_m^2 + \varepsilon_w^2 + \varepsilon_d^2} \quad (10)$$

Where ε_t is the total uncertainty of Q estimation. In this section, ε_n, ε_m, ε_w, and ε_d are the uncertainty caused by n, accuracy of CH_4 samples, wind speed, and wind direction, respectively. Results in Figure3

are used to determine the values of ε_n, ε_m, ε_w, and ε_d in each Flight.

4.Discussion

4.1.Comparison with other methods

To investigate the difference between our recommended emission model and others, three methods have been applied to estimate CH_4 emission in all Flights, including mass-balance approach, nonlinear least square fit (NLSF), and facility emission.

Mass-balance approach quantifies CH_4 emission by calculating the cross-sectional flux perpendicular to the wind direction(Krings et al. 2018). First, a two-dimensional plane is selected according to the amount of CH_4 samples. Second, the two-dimensional plane is divided into a grid of equal spatial resolution. Third, CH_4 samples are regarded as origin points to interpolate full grids defined by the Kriging interpolation scheme(Mays et al. 2009). Finally, the emission rate of the CH_4 source is calculated by

$$F_{(CH4)} = \iint v\sin(\alpha)\cdot(C_{(x,z)}-C_{bg})dxdz \quad (11)$$

Where v is the wind speed, α is the angle between wind direction and the two-dimensional plane, $C_{(x,z)}$ is the density of CH_4 in each grid, and C_{bg} is the background of CH_4 in each grid. The uncertainty analyses of this method are detailed in Nathan et al. (Nathan et al. 2015a).

NLSF and the combination of NLSF with Gaussian diffusion model are also extensively used for point-source emission retrieval (Wolff et al. 2021b; Zheng et al. 2020). In this study, NLSF is used to estimate Q in each Flight by fitting the unknown parameters in equation 1, and the uncertainty of the retrieved Q is evaluated with formula 6.

Missing date

Andersen et al. also developed an inverse Gaussian approach to quantifying CH_4 emissions from coal mine based on the same Flights (Andersen et al. 2021). First, the Gaussian dispersion is built as

$$C(x,y,z) = \frac{q}{2\pi u\sigma_y\sigma_z\cos(\theta)}\exp\left(\frac{-(y)^2}{2\sigma_y^2}\right)\left\{\exp\left(\frac{-(z-H)^2}{2\sigma_z^2}\right)+\alpha\cdot\exp\left(\frac{-(z+H)^2}{2\sigma_z^2}\right)\right\} \quad (12)$$

Where θ is the angle between the wind direction and the perpendicular line of the flight trajectory. This model does not contain the item of background of CH_4. Furthermore, σ_y and σ_z are treated as certain values in equation 8. Then, q and the related parameters are retrieved by "fmincon optimizer" in MATLAB (detailed settings are found in Andersen et al.). The CH_4 emissions in each Flight, as evaluated by Andersen et al., are presented in this section.

Facility-emission data and hourly CH_4 emission from shaft are calculated by measuring raw CH_4 concentration and air flux through the shafts. The CH_4 emission rates estimated using hourly facility-emission data for 21 August 2017 and 21 August 2017 are 14.4 ±4.9 and 8.2 ±2.9 kt/year, respectively, as shown in Figure7.

Why is the inventory emission lower for flight 8? Seems to be consistent across the second day.

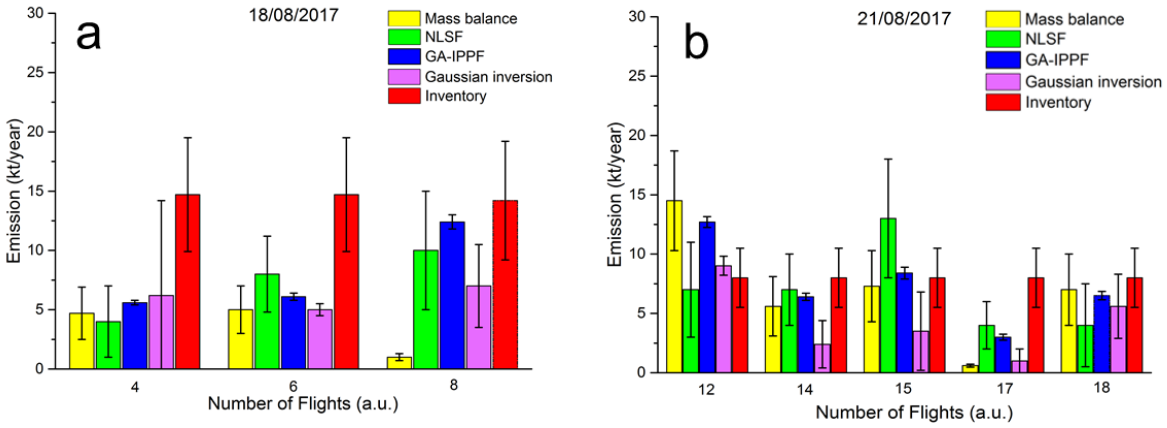

Figure7. Quantified CH_4 emission by different methods based on the collected data: (a) August 18, 2017 and (b) August 21, 2017. The results of CH_4 emission rate calculated by Mass balance and Inverse Gaussian refer to Andersen et al[30]. Why does this reference have no date and a number next to it (wrong style)

As shown in Figure7, Flights 4, 6, and 8 are measured on 18 August 2017, whereas Flights 12, 14, 15, 17, and 18 are measured on 21 August 2017. Figure7(a) shows that the CH_4-emission rates calculated by mass balance are smaller than the inventory estimation in all Flights. In Flight 8, q retrieved by mass balance is extremely lower than those quantified by other methods, whereas q retrieved by GA-IPPF model (12.4±0.6 kt/year) shows only a slight difference from the inventory. As shown in Figure 7(b), CH_4 emissions retrieved by mass balance, inverse Gaussian, and GA-IPPF model are overestimated compared with the inventory in Flight 12. Mass balance and inverse Gaussian method also show obviously underestimated q in Flight 17. Estimations of retrieved CH_4 emission in Flight 18 show consistency among methods of mass balance, GA-IPPF, and inverse Gaussian. The CH_4-emission rate of coal generally has significant variability in each measurement, even on the same day. Mass balance is very sensitive to the size settings of grids, and different height and length settings can affect the concentration distribution across the cross-section. NLSF has a high-accuracy requirement for wind measurements, and errors on these measurements have a linear influence on the final emission estimation. Notably, the standard errors of q quantified by GA-IPPF always are the least among these methods, indicating the stability of our developed model.

4.2 Application of Reanalysis meteorological database in GA-IPFF model

Wind speed and wind direction acquired by the radiosonde or weather station are two main parameters in GA-IPPF. However, additional sensors are bound to increase the cost and difficulty during actual CH_4-emission measurements. To explore the possibility of weather reanalysis data instead of actual wind measurement by sensors, we use 10 m U and V wind components from the ERA5 meteorological reanalysis database (spatial resolution is 0.1°×0.1°, and temporal resolution is 1 h) developed by the European Centre for Medium-range Weather Forecast(Hersbach et al. 2020) to evaluate GA-IPPF model. However, the wind directions from ERA obviously differ from the actual measurements during the Flights. Hence, we determine the wind direction by using the CH_4 samples, for example, the line between the shaft and the location of the maximum value of samples in the same heights is treated as the downwind direction, whose uncertainty is set as 50°. Wind speed from ERA is used for the CH_4-emission calculation, uncertainty is supposed as 2 m/s. Even oral wind speed and direction obviously differ between the two sources; however, the GA-IPPF model adjusts them into reasonable ranges. The results of q during all Flights retrieved by two meteorological data sources have been evaluated, as shown in

Table 3.

Table 3. Retrieved CH_4 emission by ERA meteorological data

Flights	Actual	ERA
4	5.6±0.2	6.0±0.3
6	6.1±0.3	6.4±0.5
8	12.4±0.6	14.4±0.9
12	12.7±0.5	13.2±0.7
14	6.4±0.3	5.0±0.4
15	8.4±0.5	7.8±0.5
17	3.0±0.3	3.4±0.5
18	6.5±0.4	7.0±0.5

Table 3 shows that the values of quantified q between two meteorological sources are within 20% in the same Flight. The standard errors of q retrieved by the ERA5 database are larger than those from actual measurements, which depends on the accuracy of the reanalysis of wind speed and wind direction. Thus, it reduces the necessity of additional equipment except for the AirCore system and the complexity of this program.

This is not a sentence

To explore the reason that the acceptable difference of calculated methane emission rate by the two sources of meteorological data. The concerned parameters in Flight 6 and Flight 15 calculated based on ERA5 meteorological data were presented in Table 4.

are

Table 4. Results calculated ERA5 meteorological data

Parameters	Flight 6	Flight 15
Oral wind speed (m/s)	2.6	4.1
Oral wind direction (°)	300	120
Emission intensity (kt/year)	6.4±0.5	7.8±0.6
Wind speed (m/s)	2.99	4.52
Wind direction (°)	349.4°	128.1
a	0.28	0.18
b	0.90	0.93
c	0.01	0.13
d	1.26	0.84
B (mg/m^3)	1.56	1.57
Emission height (m)	60.2	36.0
Reflection index	0.80	0.71

The oral wind speed and wind direction in Table 4 are obviously different from those in Table 2. However, the calculated wind directions are nearly the same based on the two sources of meteorological data. Diffusion parameters and emission height in Table 8 also show less difference in two Tables (Table 2 and Table 4). It is worth nothing that the wind speed and reflection index would be adjusted to reach the global solution by GA-IPPF model, which leads to little bias for the emission rate of CH_4 in Table 3.

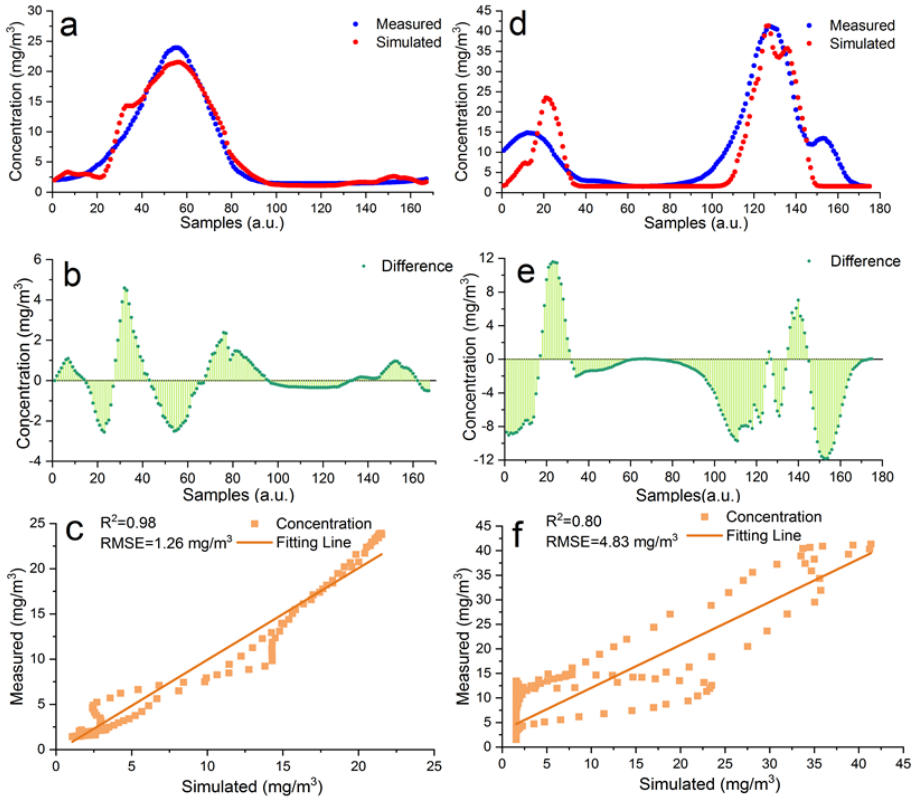

Figure8. Comparison between the measured samples and the simulated ones based on the ERA5 meteorological data: (a). Flight 6 and (d) Flight 15. The difference of simulated CH4 concentration and actual measured ones:(b) Flight 6 and (e)Flight 15. Correlation Analysis: (c) Flight 6 and (f)Flight 15.

The simulated concentration of CH_4 in Flight 6 and Flight 15 calculated by parameters in Table 4 are shown in Fig.8. In Fig.8(a), the consistency between actual samples and simulated ones is slight lower than that in Fig.6(a), D_c is ranging from -2.4 to 4.3 mg/m^3, which is an acceptable bias as only 6 points exceed 2.3 mg/m^3. R^2 (0.98) of measured samples and simulated ones is almost same to that in Fig.6(c), while RMSE is nearly three times than that in Fig.6(c). In Fig.8(d), the tendency of simulated CH_4 concentration is similar to Fig.6(d). D_c is ranging from -11.9 to 11.6 mg/m^3, which is nearly same as the result in Fig.6 (e), it is worth nothing that D_c simulated by ERA meteorological data is slight larger on samples (NO.1 to 20) compared with that in Fig.6 (e). The R^2 and RMSE in Fig. 8(f) indicate that the retrieved results using ERA data are less accurate than that using actual measured meteorological data. In summary, though we set large uncertainties in ERA meteorological data, GA-IPPF can still guarantee reasonable and adequate accuracy for the retrieved emission rate and diffusion parameters.

5.Conclusion

CH_4 emissions from coal are inconsistent even with short time differences. They usually show a large difference for different mining volumes and types. Enhancement in CH_4 by the emission source is much larger than the background concentration, and the distribution of leak gas shows an obvious spatial difference. Hence, the retrieval time needs to be shortened for each emission measurement. AirCore has high portability and flexibility to measure CH_4 concentration around emission sources, accompanied by the GA-IPPF model, which is acceptable to calculate CH_4 emission from coals or other point sources. This program can help improve the accuracy of estimating CH_4 emission from coals, especially developed countries that even lack no inventories of gas emission. It can also help governments evaluate

Pipes leak, this is a fugitive vent emission

this is a double negative

the fugitive CH_4-emission rate during mining and formulate policies to promote the innovation of mining equipment and technology. The recommended program is appropriate for quantifying local sources based on the advantage of hardware and retrieval model. The UAV-based AirCore system helps rebuild the diffusion of CH_4 with flexibility and high sampling rate. The GA model could restrict the calculated emission details within a reasonable range. Therefore, this program has great potential application in the point-source quantitation of other gases, such CO_2, SO_2, etc.

Should include a recommendation of how many Air Core retrievals from a single point source are required to mininmise the errors on model results

Acknowledgements

This work was supported by the National Natural Science Foundation of China (Grant No.41971283, 41801261, 41827801, 41901274, 41801282, 42171464), the National Key Research and Development Program of China (2017YFC0212600), The Key Research and Development Project of Hubei Province (2021BCA216), the Open Research Fund of National Earth Observation Data Center(NODAOP2021005).

References Need complete references, add journal volume numbers and pages / DOI where missing

Allen, G., Hollingsworth, P., Kabbabe, K., Pitt, J.R., Mead, M.I., Illingworth, S., Roberts, G., Bourn, M., Shallcross, D.E., & Percival, C.J. (2018). The development and trial of an unmanned aerial system for the measurement of methane flux from landfill and greenhouse gas emission hotspots. *Waste Management*, S0956053X17309698

Andersen, T., Scheeren, B., Peters, W., & Chen, H.L. (2018). A UAV-based active AirCore system for measurements of greenhouse gases. *Atmospheric Measurement Techniques, 11*, 2683-2699

Andersen, T., Vinkovic, K., de Vries, M., Kers, B., Necki, J., Swolkien, J., Roiger, A., Peters, W., & Chen, H. (2021). Quantifying methane emissions from coal mining ventilation shafts using an unmanned aerial vehicle (UAV)-based active AirCore system. *Atmospheric Environment: X, 12*

Cardoso-Saldana, F.J., & Allen, D.T. (2020). Projecting the Temporal Evolution of Methane Emissions from Oil and Gas Production Sites. *Environ Sci Technol, 54*, 14172-14181

Caulton, D.R., Qi, L., Bou-Zeid, E., Lu, J., Zondlo, M.A.J.A.C., & Physics (2017). Improving Mobile Platform Gaussian-Derived Emission Estimates Using Hierarchical Sampling and Large Eddy Simulation, 1-39

Elder, C.D., Thompson, D.R., Thorpe, A.K., Hanke, P., Walter Anthony, K.M., & Miller, C.E. (2020). Airborne Mapping Reveals Emergent Power Law of Arctic Methane Emissions. *Geophysical Research Letters, 47*

Feng, L., Palmer, P.I., B?Sch, H., Parker, R.J., Webb, A.J., Correia, C.S.C., Deutscher, N.M., Domingues, L.G., Feist, D.G., Gatti, L.V.J.A.C., & Physics (2016). Consistent regional fluxes of CH4 and CO2 inferred from GOSAT proxy XCH4 : XCO2 retrievals, 2010-2014*, 17*, 1-33

Guanter, L., Irakulis-Loitxate, I., Gorrono, J., Sanchez-Garcia, E., Cusworth, D.H., Varon, D.J., Cogliati, S., & Colombo, R. (2021). Mapping methane point emissions with the PRISMA spaceborne imaging spectrometer. *Remote Sensing of Environment, 265*

Hersbach, H., Bell, B., Berrisford, P., Hirahara, S., Horanyi, A., Munoz-Sabater, J., Nicolas, J., Peubey, C., Radu, R., Schepers, D., Simmons, A., Soci, C., Abdalla, S., Abellan, X., Balsamo, G., Bechtold, P., Biavati, G., Bidlot, J., Bonavita, M., De Chiara, G., Dahlgren, P., Dee, D., Diamantakis, M., Dragani, R., Flemming, J., Forbes, R., Fuentes, M., Geer, A., Haimberger, L., Healy, S., Hogan, R.J., Holm, E., Janiskova, M., Keeley, S., Laloyaux, P., Lopez, P., Lupu, C., Radnoti, G., de Rosnay, P., Rozum, I., Vamborg, F., Villaume, S., & Thepaut, J.N. (2020). The ERA5 global reanalysis. *Quarterly Journal Of the Royal Meteorological Society, 146*, 1999-2049

Iwaszenko, S., Kalisz, P., Slota, M., & Rudzki, A. (2021). Detection of Natural Gas Leakages Using a

Laser-Based Methane Sensor and UAV. *Remote Sensing, 13*
Krings, T., Neininger, B., Gerilowski, K., Krautwurst, S., Buchwitz, M., Burrows, J.P., Lindemann, C., Ruhtz, T., Schuttemeyer, D., & Bovensmann, H. (2018). Airborne remote sensing and in situ measurements of atmospheric CO2 to quantify point source emissions. *Atmospheric Measurement Techniques, 11*, 721-739
Liu, D., & Michalski, K.A. (2016). Comparative study of bio-inspired optimization algorithms and their application to dielectric function fitting. *Journal of Electromagnetic Waves and Applications, 30*, 1885-1894
Liu, F., Duncan, B.N., Krotkov, N.A., Lamsal, L.N., Beirle, S., Griffin, D., McLinden, C.A., Goldberg, D.L., & Lu, Z.F. (2020). A methodology to constrain carbon dioxide emissions from coal-fired power plants using satellite observations of co-emitted nitrogen dioxide. *Atmospheric Chemistry and Physics, 20*, 99-116
Mays, K.L., Shepson, P.B., Stirm, B.H., Karion, A., Sweeney, C., & Gurney, K.R. (2009). Aircraft-Based Measurements of the Carbon Footprint of Indianapolis. *Environmental Science & Technology, 43*, 7816-7823
Nathan, B.J., Golston, L.M., O'Brien, A.S., Ross, K., Harrison, W.A., Tao, L., Lary, D.J., Johnson, D.R., Covington, A.N., & Clark, N.N. (2015a). Near-Field Characterization of Methane Emission Variability from a Compressor Station Using a Model Aircraft. *Environmental Science & Technology, 49*, 7896-7903
Nathan, B.J., Golston, L.M., O'Brien, A.S., Ross, K., Harrison, W.A., Tao, L., Lary, D.J., Johnson, D.R., Covington, A.N., Clark, N.N., & Zondlo, M.A. (2015b). Near-Field Characterization of Methane Emission Variability from a Compressor Station Using a Model Aircraft. *Environ Sci Technol, 49*, 7896-7903
Pan, G., Xu, Y., & Huang, B. (2021). Evaluating national and subnational CO2 mitigation goals in China's thirteenth five-year plan from satellite observations. *Environ Int, 156*, 106771
Robertson, A.M., Edie, R., Snare, D., Soltis, J., Field, R.A., Burkhart, M.D., Bell, C.S., Zimmerle, D., & Murphy, S.M. (2017). Variation in Methane Emission Rates from Well Pads in Four Oil and Gas Basins with Contrasting Production Volumes and Compositions. *Environmental Science & Technology, 51*, 8832-8840
Schneising, O., Buchwitz, M., Reuter, M., Vanselow, S., Bovensmann, H., & Burrows, J.P. (2020). Remote sensing of methane leakage from natural gas and petroleum systems revisited. *Atmospheric Chemistry and Physics, 20*, 9169-9182
Shah, A., Pitt, J.R., Ricketts, H., Leen, J.B., & Allen, G. (2019). Testing the near-field Gaussian plume inversion flux quantification technique using unmanned aerial vehicle sampling
Shi, T., Han, G., Ma, X., Zhang, M., Pei, Z., Xu, H., Qiu, R., Zhang, H., & Gong, W. (2020a). An inversion method for estimating strong point carbon dioxide emissions using a differential absorption Lidar. *Journal of Cleaner Production, 271*
Shi, T.Q., Ma, X., Han, G., Xu, H., Qiu, R.N., He, B., & Gong, W. (2020b). Measurement of CO2 rectifier effect during summer and winter using ground-based differential absorption LiDAR. *Atmospheric Environment, 220*, 10
Tu, Q.S., Hase, F., Schneider, M., Garcia, O., Blumenstock, T., Borsdorff, T., Frey, M., Khosrawi, F., Lorente, A., Alberti, C., Bustos, J.J., Butz, A., Carreno, V., Cuevas, E., Curcoll, R., Diekmann, C.J., Dubravica, D., Ertl, B., Estruch, C., Leon-Luis, S.F., Marrero, C., Morgui, J.A., Ramos, R., Scharun, C., Schneider, C., Sepulveda, E., Toledano, C., & Torres, C. (2022). Quantification of CH4 emissions from waste disposal sites near the city of Madrid using ground- and space-based observations of COCCON,

TROPOMI and IASI. *Atmospheric Chemistry and Physics, 22*, 295-317

Varon, D.J., Jacob, D.J., Jervis, D., & McKeever, J. (2020). Quantifying Time-Averaged Methane Emissions from Individual Coal Mine Vents with GHGSat-D Satellite Observations. *Environmental Science & Technology, 54*, 10246-10253

Varon, D.J., McKeever, J., Jervis, D., Maasakkers, J.D., Pandey, S., Houweling, S., Aben, I., Scarpelli, T., & Jacob, D.J. (2019). Satellite Discovery of Anomalously Large Methane Point Sources From Oil/Gas Production. *Geophysical Research Letters, 46*, 13507-13516

Venkatram, A. (1996). An examination of the Pasquill-Gifford-Turner dispersion scheme. *Atmospheric Environment, 30*, 1283-1290

Wolff, S., Ehret, G., Kiemle, C., Amediek, A., Quatrevalet, M., Wirth, M., & Fix, A. (2021a). Determination of the emission rates of CO2 point sources with airborne lidar. *Atmos. Meas. Tech., 14*, 2717-2736

Wolff, S., Ehret, G., Kiemle, C., Amediek, A., Quatrevalet, M., Wirth, M., & Fix, A. (2021b). Determination of the emission rates of CO₂ point sources with airborne lidar. *Atmospheric Measurement Techniques, 14*, 2717-2736

Zhang, Y., Gautam, R., Pandey, S., Omara, M., Maasakkers, J.D., Sadavarte, P., Lyon, D., Nesser, H., Sulprizio, M.P., Varon, D.J., Zhang, R., Houweling, S., Zavala-Araiza, D., Alvarez, R.A., Lorente, A., Hamburg, S.P., Aben, I., & Jacob, D.J. (2020). Quantifying methane emissions from the largest oil-producing basin in the United States from space. *Sci Adv, 6*, eaaz5120

Zheng, B., Chevallier, F., Ciais, P., Broquet, G., Wang, Y., Lian, J., & Zhao, Y. (2020). Observing carbon dioxide emissions over China's cities and industrial areas with the Orbiting Carbon Observatory-2. *Atmospheric Chemistry And Physics, 20*, 8501-8510

Zhou, X.C., Yoon, S.J., Mara, S., Falk, M., Kuwayama, T., Tran, T., Cheadle, L., Nyarady, J., Croes, B., Scheehle, E., Herner, J.D., & Vijayan, A. (2021). Mobile sampling of methane emissions from natural gas well pads in California. *Atmospheric Environment, 244*